Structure, Vol. 8, 1105–1113, November, 2000, ©2000 Elsevier Science Ltd. All rights reserved. PII S0969-2126(00)00516-5

Structure of the Tie2 RTK Domain: Self-Inhibition by the Nucleotide Binding Loop, Activation Loop, and C-Terminal Tail

Lisa M. Shewchuk,* Anne M. Hassell, Byron Ellis, W. D. Holmes, Roderick Davis, Earnest L. Horne, Sue H. Kadwell, David D. McKee, and John T. Moore
GlaxoWellcome
Research Triangle Park, North Carolina 27709

Summary

Background: Angiogenesis, the formation of new vessels from the existing vasculature, is a critical process during early development as well as in a number of disease processes. Tie2 (also known as Tek) is an endothelium-specific receptor tyrosine kinase involved in both angiogenesis and vasculature maintenance.

Results: We have determined the crystal structure of the Tie2 kinase domain to 2.2 Å resolution. The structure contains the catalytic core, the kinase insert domain (KID), and the C-terminal tail. The overall fold is similar to that observed in other serine/threonine and tyrosine kinase structures; however, several unique features distinguish the Tie2 structure from those of other kinases. The Tie2 nucleotide binding loop is in an inhibitory conformation, which is not seen in other kinase structures, while its activation loop adopts an "activated-like" conformation in the absence of phosphorylation. Tyr-897, located in the N-terminal domain, may negatively regulate the activity of Tie2 by preventing dimerization of the kinase domains or by recruiting phosphatases when it is phosphorylated.

Conclusion: Regulation of the kinase activity of Tie2 is a complex process. Conformational changes in the nucleotide binding loop, activation loop, C helix, and the C-terminal tail are required for ATP and substrate binding.

Introduction

Vasculogenesis and angiogenesis are critical processes in embryonic development as well as in a number of diseases, including ischemic coronary artery disease, cancer, diabetic retinopathy, and rheumatoid arthritis [1–7]. While the precise molecular mechanisms that regulate these processes have not been fully elucidated, normal vascular development is known to be dependent on the function of several endothelium-specific receptor tyrosine kinases (RTKs) (reviewed in [8] and [9]). These include the TIE RTKs, Tie1 and Tie2 (or Tek), as well as the vascular endothelial growth factor receptor kinases (VEGFRs) [1–4]. The VEGFRs are believed to play an early role in these processes by directing the differentiation of mesodermal cells into endothelial cells and the proliferation and migration of endothelial cells to form primitive tubular vessels [10–12]. The TIE RTKs are involved in the later stages of modulating cell–cell and cell–matrix interactions required for vascular remodeling and maturation [13, 14].

Receptor tyrosine kinases comprise an extracellular ligand binding domain and an intracellular kinase domain. Binding of extracellular ligand is believed to promote dimerization, which leads to autophosphorylation and activation of the kinase domain [reviewed in 15]. Stringent regulation of the phosphorylation state and activity of the Tie2 kinase domain is crucial to normal vasculature development and maintenance. Tie2 activity is precisely regulated by the opposing actions of agonistic and antagonistic extracellular ligands [16–18]. Tie2 activation requires autophosporylation in response to binding its agonists angiopoietin 1 (Ang1) and Ang4, whereas inactivation occurs in response to Ang2 and Ang3. Tie2 mutations, which result in ligand-independent and enhanced autophosphorylation, cause hereditary venous malformations [19, 20]. Conversely, transgenic mice that express a kinase-inactive form of Tie2 or Tie2 null mice die in utero due to defects in their microvasculature [21, 22]. Inactivation of Ang1 or overexpression of Ang2 produces similar defects [17, 23, 24].

The broad clinical potential of antiangiogenic therapy is just now being realized. Inhibition of either VEGFR2 or Tie2 by small molecules, antibodies generated against the extracellular domain, and gene therapy have been shown to reduce tumor progression [11, 25]. Therefore, the three-dimensional structure of the kinase domain of these receptors will enhance the design of potent and selective small-molecule inhibitors as therapeutic agents. To this end, we have determined the crystal structure of the Tie2 kinase domain to a 2.2 Å resolution. The structure contains the catalytic core, the kinase insert domain (KID), and the C-terminal tail. Several unique features distinguish this structure from those of other receptor tyrosine kinases whose structures are known [26–29]. Most notably, the Tie2 nucleotide binding loop is in an inhibitory conformation, which is not seen in other RTKs, while its activation loop adopts an "activated-like" conformation in the absence of phosphorylation.

Results and Discussion

Structure Determination

The cytoplasmic kinase domain of Tie2 (Tie2K), residues 808–1124, was expressed in baculovirus-infected insect cells. The first 35 cytoplasmic residues (juxtamembrane) were not included in the construct, and a 6-histidine tag was added at the N terminus for purification purposes. Baculovirus-expressed Tie2K was heterogeneous with respect to phosphorylation. Typically, preparations contained a mixture of proteins with 0–6 phosphoryl groups that could not be fully separated by standard chromatographic procedures. Crystallization screens were initially performed using a mixture of the non-, mono-, and diphosphorylated species. Three different crystal forms of Tie2K were obtained; crystal forms I and II contained nonphosphorylated protein, while crystal form III contained monophosphorylated protein (Table 1).

A mutant form of Tie2K provided a fourth crystal form. Two major phosphorylation sites and one minor site were mapped by mass spectrometry. The two major sites, Y897 and S1119, were mutated to phenylalanine and alanine, respectively, while

*To whom correspondence should be addressed (e-mail: lms18808@glaxowellcome.com).

Key words: tyrosine kinase; Tek; angiogenesis; X-ray structure; kinase insert domain; signal transduction

Table 1. Crystal and Data Statistics

Crystal form	I	II	III	IV
Space Group	$P2_1$	$P2_12_12_1$	$P2_12_12_1$	$C222_1$
Unit cell a (Å)	66	79	52	95
Unit cell b (Å)	92	92	78	114
Unit cell c (Å)	70	109	79	78
Unit cell β (°)	108	90	90	90
Mol/asu	2	2	1	1
Resolution (Å)	2.2	2.5	2.2	2.1
R_{sym}[a,b] (%)	7.5 (20)	11 (29)	7.9 (23)	7.8 (25)
Completeness[b] (%)	96 (95)	98 (98)	99 (96)	98 (88)
R_{cryst}[c] (%)	19	21	20	21
R_{free}[d] (%)	23	26	23	24
Number of nonhydrogen protein atoms	4766	4766	2368	2375
Number of solvent molecules	361	188	170	200
Rmsd from ideal				
Bond lengths (Å)	0.0058	0.0063	0.0064	0.0060
Bond angles (°)	1.15	1.16	1.19	1.15

[a] $R_{sym} = \Sigma_{hkl}|I - <I>|I\Sigma I$, where I is the observed intensity and $<I>$ is the average intensity from observations of symmetry-related reflections.
[b] Value in parentheses is for the highest resolution shell.
[c] $R_{cryst} = \Sigma_{hkl}||F_{obs}| - |F_{calc}||/\Sigma|F_{obs}|$, where F_{obs} and F_{calc} are the observed and calculated structure factor amplitudes, respectively, for the *hkl* reflections.
[d] R_{free} is calculated for a set of reflections that were not included in atomic refinement.

the minor site, Y1048, was mutated to phenylalanine. The mutant form of Tie2K was purified to homogeneity as unphosphorylated protein and gave rise to crystal form IV (Table 1).

The structure of crystal form I was solved by molecular replacement using the structure of the unphosphorylated kinase domain of fibroblast growth factor receptor 1 (FGFR1) [28] as a search model. The structure was refined to an R factor of 19% at 2.2 Å resolution. Six residues at the N terminus, three residues at the C terminus, four residues in the activation loop, and six residues connecting β3 and αC were disordered and could not be modeled. The structures of crystal forms II, III, and IV were solved by molecular replacement using the structure determined for crystal form I. The Tie2K structure in all four crystal forms was essentially identical, and this result suggests that conformations observed in the structure are not due to crystal packing forces. Residues disordered in crystal form I were also disordered in crystal forms II, III, and IV. Superposition of all C_αs yielded root mean square deviations (rmsd) of 0.18 Å, 0.47 Å, and 0.45 Å for I versus II, I versus III, and I versus IV, respectively.

Overview of the Structure

The overall architecture of Tie2K was analogous to structures reported previously for both serine/threonine and tyrosine protein kinases (reviewed in [30] and [31]). A C_α trace of Tie2K is shown in Figure 1, where kinase secondary structural elements are labeled according to the convention originally given for cAPK [32]. Tie2K folds into two domains, with catalysis occurring in a cleft between the two domains. Residues in the N-terminal domain are primarily responsible for ligating ATP, while residues in the C-terminal domain are involved in catalysis and substrate binding.

The N-terminal domain (residues 808–904) folds into a twisted β sheet and an α helix. The larger C-terminal domain (residues 905–1124) contains seven α helices (αD–αI) and two sets of anti-parallel β strands (β7/β8 and β9/β10). Strands 7 and 8 are positioned at the interdomain interface adjacent to the N-terminal β sheet. The kinase insert domain comprises two short helical segments that pack against the C-terminal lobe and the extended C-terminal tail. Like other kinases, Tie2K also contains functionally important loop regions: the glycine-rich nucleotide binding loop (residues 831–836), the catalytic loop (residues 962–968), and the activation loop (residues 982–1008), all of which will be described in further detail below.

Comparison to FGFR1

Of the reported kinase structures, the overall structure of Tie2K most closely resembles the catalytic domain of FGFR1, with

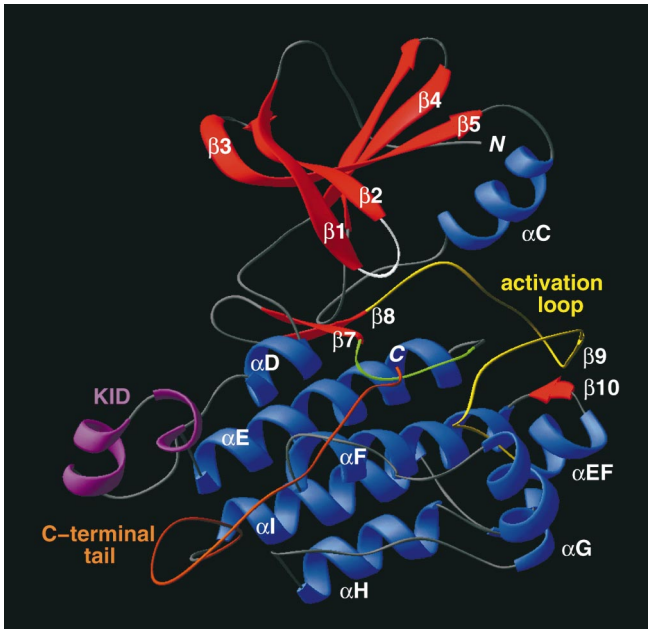

Figure 1. Overall Fold of Tie2K

Ribbon diagram of the Tie2K structure. The α helices are blue, the β strands are red, the nucleotide binding loop is white, the catalytic loop is green, the activation loop is yellow, the KID is pink, and the C-terminal tail is orange. The termini are denoted by N and C. Breaks in the chain occur between β3 and helix C and in the activation loop due to crystal disorder. The figure was prepared with RIBBONS [45].

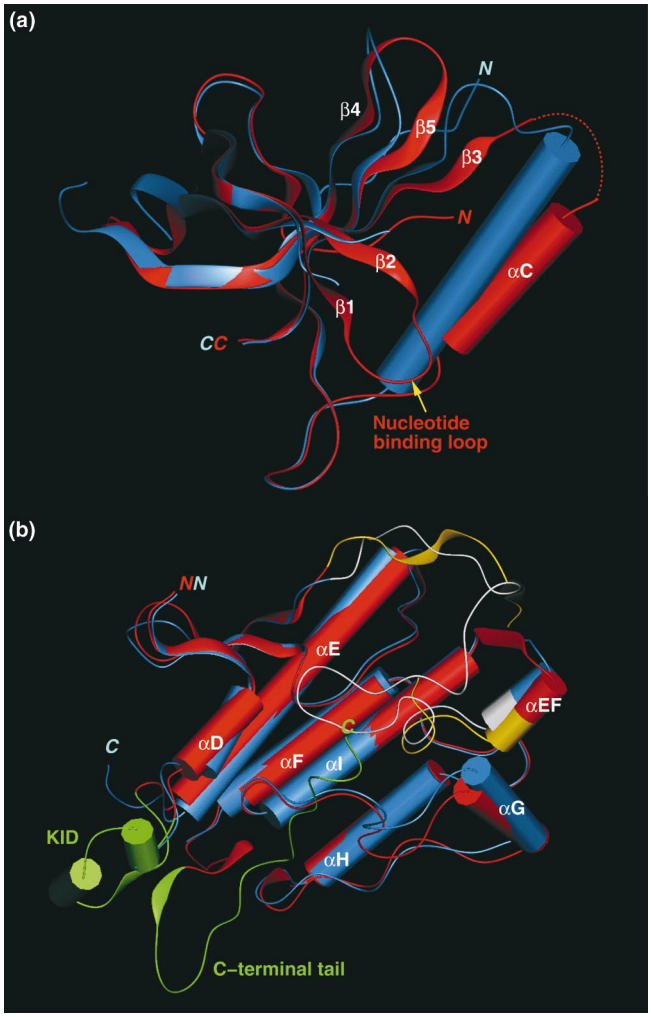

Figure 2. Superposition of the N- and C-Terminal Domains of Tie2K and FGFR1

(A) Ribbon diagram of the N-terminal domains of Tie2K and FGFR1 in which the C_αs of the β sheets have been superimposed. Tie2K is shown in red, and FGFR1 is shown in blue. The dashed line indicates the position of the disordered loop connecting β3 and helix C in Tie2K.

(B) Ribbon diagram of the C-terminal domains of Tie2K and FGFR1 in which the C_αs of the α helices have been superimposed. Tie2K is shown in red, and FGFR1 is shown in blue. The activation loops for Tie2K and FGFR1 are shown in yellow and white, respectively. The C-terminal tail and KID for Tie2K are shown in green. Figures were prepared with QUANTA [43].

which it shares approximately 45% sequence identity [28]. Superposition of the five β strands in the N-terminal domains of Tie2K and FGFR1 yielded an N-terminal domain C_α rmsd of 0.76 Å; superposition of the C-terminal domains using C_αs from the seven α helices gave a C-terminal domain C_α rmsd of 0.58 Å. Like unphosphorylated FGFR1, Tie2K is in an opened conformation with a relative rotation of approximately 15° between the N- and C-terminal lobes when compared to the closed, active structure of the insulin receptor kinase (IRK) [27].

The β sheet topologies in the N-terminal domain of FGFR1 and Tie2K are quite similar (Figure 2A). However, significant differences are observed in the nucleotide binding loop, the loops connecting β3 to αC and β4 to β5, and the C helix position. In Tie2K, β strands 3, 4, and 5 contain one additional residue compared with FGFR1, and this extra residue produces a change in the conformation of the loop regions connecting these β sheets. That extension of the β3-β4-β5 sheet displaces residues in the C helix by 2.5–5.5 Å from their equivalent positions in FGFR1. In addition, six Tie2K residues in the loop connecting β3 with αC (A861–H866) are disordered in all four crystal forms. Therefore, only three and a half turns of this helix are observed for Tie2K as opposed to five for FGFR1.

In the N-terminal domain of kinases, two conserved, charged residues form a salt bridge to correctly position the α- and β-phosphates of ATP for catalysis. In Tie2K these residues correspond to K855 on β3 and E872 on αC. Due to the shift in αC, these residues are approximately 7.2 Å apart compared with the approximately 3–4 Å distance observed in other kinase structures [26–29]. While the shift in αC is not as dramatic as observed in the structures of inactive cdk2 versus the activated cdk2/cyclinA complex (8.5 Å) [33], the conformational change required to bring these residues into proper alignment for ATP binding is not obvious.

The C-terminal lobes of Tie2K and FGFR1 are also quite similar (Figure 2B) except for the positions of the activation loops (see below) and the KID, which is disordered in FGFR1. The C-terminal tail was included in our Tie2K construct but not in FGFR1, IRK, or VEGFR2 and is observed in the crystal structure presented here. This tail has an extended conformation that packs under the KID, runs along αI, F, and E, and ends near the substrate binding site.

Activation Loop and Catalytic Residues

Protein kinases contain a large flexible loop, called the activation loop or A-loop, whose conformation is believed to regulate kinase activity. In many kinases, the conformation of the A-loop is controlled by the phosphorylation of specific residues within this region [30]. The activation loop generally begins with a conserved Asp-Phe-Gly sequence (Tie2K 982–984) and ends at a conserved Ala-Pro-Glu (Tie2K 1006–1008) [30]. In structures of inactive kinases, this loop often blocks either the substrate or the ATP binding sites [26, 28, 29]. Upon phosphorylation, the A-loop is repositioned to contact residues in the C-terminal domain [27]. The activating phosphate can then interact with a cluster of basic residues that include a conserved arginine (Tie2K R963) that precedes the catalytic aspartate (Tie2K D964). The aspartyl residue of the Asp-Phe-Gly motif ligates a Mg^{2+} ion, which in turn contacts the β- and γ-phosphates of ATP.

In Tie2K the activation loop corresponds to residues 982–1008 and contains a single tyrosine at position 992. The conserved Ala-Pro-Glu sequence is Ala-Ile-Glu in Tie2. In the Tie2K structure presented here, the A-loop more closely resembles that of activated IRK than that seen for inactive, unphosphorylated FGFR1 (Figure 3). Four residues (T996–R999) near the C-terminal end of Tie2K's A-loop are disordered. All attempts to autophosphorylate Y992 in the activation loop using purified wild-type protein have been unsuccessful. However, when tyrosines 897 and 1048 and serine 1119 were mutated to phenylalanine and alanine, respectively, the purified protein could be quantitatively phosphorylated on Y992. These observations suggest that the mode by which Tie2 is activated is complex and may differ from that found with other RTKs [30].

The conformation of the conserved Asp-Phe-Gly motif of the activation loop is also significantly different than that seen in other kinase structures [26–29]. The side chains of D982 and

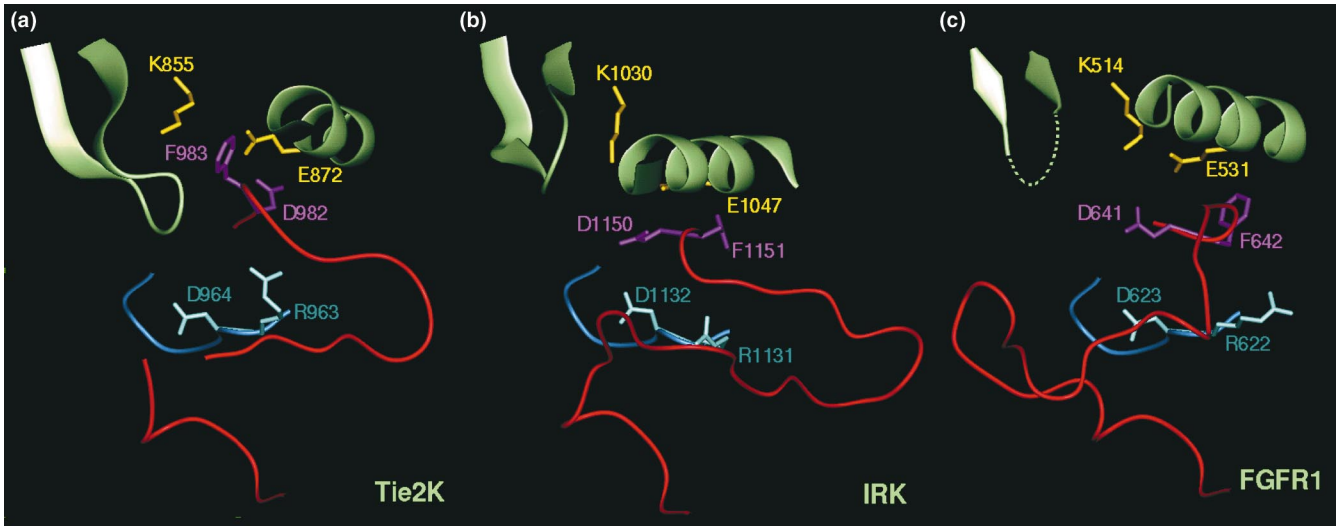

Figure 3. Activation, Nucleotide Binding, and Catalytic Loops in Tie2K, Unphosphorylated FGFR1, and Activated IRK

The nucleotide binding loop and helix C are shown in green, the activation loop is shown in red, and the catalytic segment is shown in blue. The lysine and glutamic acid residues that form a salt bridge are shown in yellow. The aspartate and arginine of the catalytic HDRLAAR motif are shown in blue, while the aspartate and phenylalanine of the Asp-Phe-Gly motif at the beginning of the activation loop are shown in pink. Loops disordered in the crystal structures are indicated by dashed lines. The figures were generated using QUANTA.

F983 point in directions opposite to those observed in non-phosphorylated FGFR1 and activated IRK (Figure 3). The D982 side chain is directed toward the back of the pocket and away from the ATP binding site. The Tie2K side chain of F983 extends toward the solvent and is sandwiched between the side chains of K855 of β3 and E872 of αC, the conserved residues that form the salt bridge required to correctly position the phosphates of ATP. Although the Tie2K activation loop adopts an "active-like" conformation overall, the Asp-Phe-Gly motif at the beginning of this loop has a conformation that could inhibit ATP binding.

The catalytic loop of protein kinases lies between αE and β7 and contains an invariant aspartic acid (D964 in Tie2) that serves as the catalytic base in the phosphotransfer reaction [30]. The catalytic loops of Tie2, FGFR1, VEGFR2, and IRK are identical in sequence: His-Arg-Asp-Leu-Ala-Ala-Arg-Asn [26, 28, 29]. In Tie2K, the backbone and side chain positions of this loop are similar to those in the unliganded FGFR1 and VEGFR2 and in the ternary phosphorylated IRK complex structures (Figure 3).

Nucleotide Binding Loop

The nucleotide binding loop contains residues responsible for binding the triphosphate moeity of ATP in the correct position for catalysis [30]. This glycine-rich loop is believed to be quite flexible and is often either disordered or has high B factors in many unliganded kinase structures [28, 29].

In Tie2K, this loop adopts a unique self-inhibitory conformation with residues 832–836 occupying the ATP binding site (Figure 4). The γ carboxylate of E832, if protonated, could form a hydrogen bond with the backbone carbonyl of E903. The backbone carbonyl of E903 presumably participates in the binding of ATP through a hydrogen bond to the 6 amino group of the nucleotide. The α- and β-phosphate binding sites of ATP are occupied by N834 and G836. F835 sits in a pocket at the back of the site formed by the side chains of K855, I886, I902, and F983. N834 occupies the site of the conserved aspartate of the Asp-Phe-Gly motif located in the A-loop. This conserved aspartate binds Mg^{2+} and the γ-phosphate of ATP. The conformation of the nucleotide binding loop is further stabilized by hydrogen bonds between the backbone carbonyl of F835 and the NZ of K855, the backbone NH of N834 and OD1 of N969, and OD1 of N834 and the backbone NH of F983.

The unusual conformation of the nucleotide binding loop in Tie2K cannot readily be explained on the basis of primary sequence. Sequence comparisons between Tie2K and other serine/threonine and tyrosine kinases do not reveal any unique residues in Tie2K.

ATP was modeled into the active site of Tie2K based on the structure of activated IRK. As seen in Figure 4, the nucleotide binding loop precludes binding of ATP. In agreement with and predicted by the Tie2K structure, we have not been successful in soaking ATP into existing crystals or cocrystallizing this kinase with ATP.

Kinase Insert Domain

Many RTKs contain an insert of variable length and sequence between αD and αE in their C-terminal domain. This insert can be as short as 12 or as long as 97 residues, as in IRK and the platelet-derived growth factor receptor β (PDGFRβ), respectively [26, 34]. Deletion or mutation of this region in other kinases revealed that the KID is not necessary for intrinsic kinase activity [29, 34, 35]. However, this KID may be important for protein–protein interactions involved in signal transduction via autophosphorylation of KID tyrosine residues [34, 35]. In Tie2, this region corresponds to residues 916–936 and does not contain tyrosine residues. Its function, if any, is not known.

Due to the lack of sequence conservation in this domain, structural conservation is also not expected. In FGFR1, the KID is apparently quite mobile and disordered in the crystal structure of the unliganded protein [28]. In VEGFR2, the KID was deleted in the construct used for structural studies [29]. In the IRK structure, this region, P1093-G1100, is proline rich and forms a loop that folds toward the N-terminal domain [26]. In Tie2K, the KID consists of two short helical segments

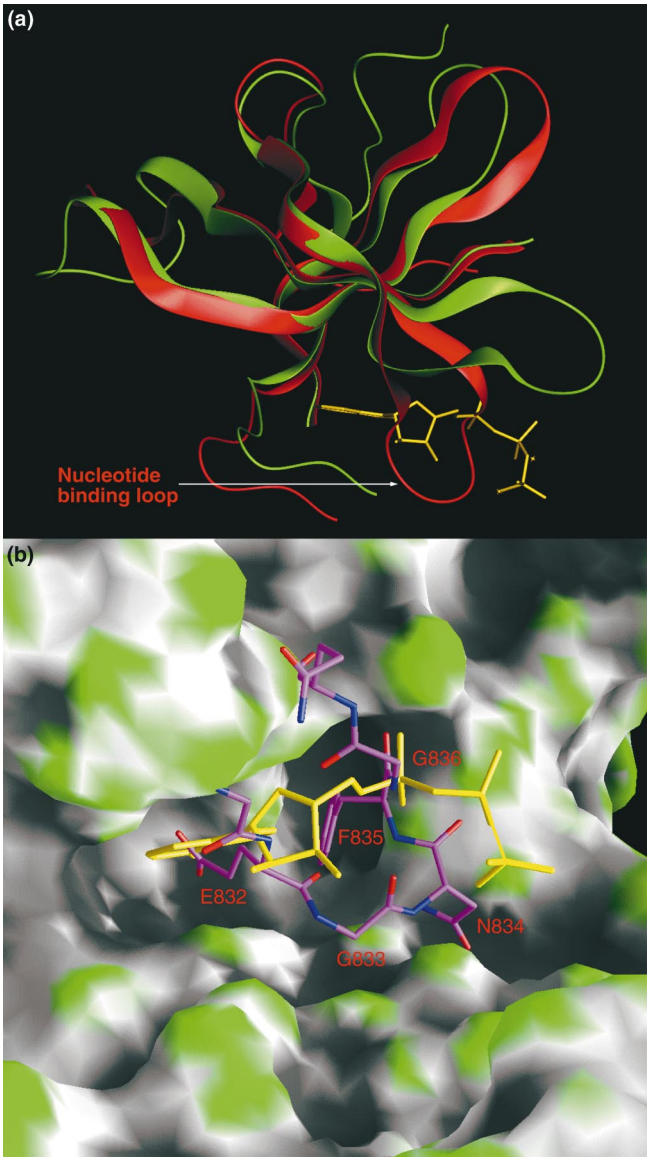

Figure 4. ATP Binding Site

(A) Superposition of the N-terminal β sheets of Tie2K and activated IRK C_αs of β1–β5 were used to superimpose the structures of Tie2K and activated IRK (PDB entry 1IR3). Tie2K is shown in red, IRK is shown in green, and ATP from the IRK structure is shown in yellow. The figure was prepared with QUANTA.

(B) Surface representation of the ATP binding site of Tie2K. The nucleotide binding loop is shown as a purple stick figure. The position of ATP, based on the superposition in Figure 5A, is shown in yellow. The figure was prepared with GRASP [46].

connected by a turn, as shown in Figure 5, and packs against residues 1104–1112 in the C-terminal tail.

C-Terminal Tail: Interaction with Accessory Proteins

The C-terminal tail of Tie2 has been shown to bind a number of proteins containing src homology 2 (SH2) and phosphotyrosine binding (PTB) domains in a phosphotyrosine-dependent manner. Numerous reports suggest that tyrosines 1101 and 1112 in the C-terminal tail interact with the SH2 domains of Grb2,

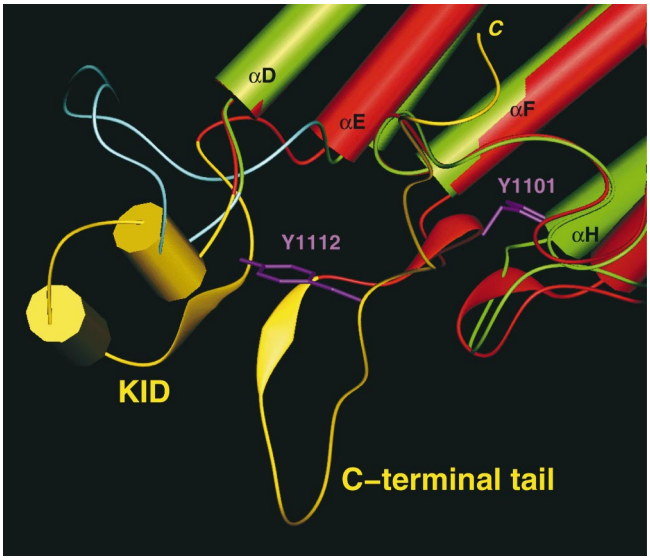

Figure 5. Kinase Insert Domain and C-Terminal Tail

Ribbon diagram of the KIDs of Tie2K and IRK in which the C_αs of the C-terminal domain α helices have been superimposed. Tie2K is shown in red, and IRK is shown in green. The KID and C-terminal tail for Tie2K is shown in yellow. The KID for IRK is shown in blue. Y1101 and Y1112 are highlighted in purple. Figures were prepared with QUANTA.

Grb7, Grb14, Shp2, the p85 subunit of PI3 kinase, and the PTB domain of Dok-R [36–40].

In our unliganded crystal structure, the hydroxyls of Y1101 and Y1112 are not solvent exposed and appear to play a structural role (Figure 5). The hydroxyl of Y1101 hydrogen bonds to the side chain of E759, while the phenyl ring is packed between the side chains of M757 and K762. The hydroxyl of Y1112 hydrogen bonds to the main chain NH and carbonyl oxygen of L579 and A592, respectively. The phenyl ring of Y1112 sits in a hydrophobic pocket formed by the side chains of L696, L579, F1114, and R577. Mass spectrometric analysis of the baculovirus-expressed Tie2K found that Y897 and Y1048, which point directly out into solvent, are partially phosphorylated. There was no evidence for phosphorylation of Y1101 or Y1112.

In the unphosphorylated FGFR1 and IRK structures, the activation loop blocks access to the substrate binding site [26, 28]. In Tie2K, the activation loop adopts an "active-like" conformation, while the end of the C-terminal tail could block access to the substrate binding site. In the structure presented here, the last three residues of the C-terminal tail are disordered. The last ordered residue of the C-terminal tail, E1120, forms a salt bridge with R915 and is positioned near the peptide binding site in the activated IRK-peptide complex (Figure 6). Therefore, these data suggest that with the Tie2K construct used in these structural studies, the C-terminal tail must undergo a conformational change upon activation of the protein and expose both the substrate binding site and Y1101 and Y1112 for phosphorylation and signaling.

Mutational Analysis – Vascular Dysmorphogenesis

Two mutations in the N-terminal domain of Tie2, R849W and Y897S, segregate with an autosomal dominant condition referred to as vascular dysmorphogenesis [19, 20]. This condition is characterized by lesions consisting of haphazardly arranged,

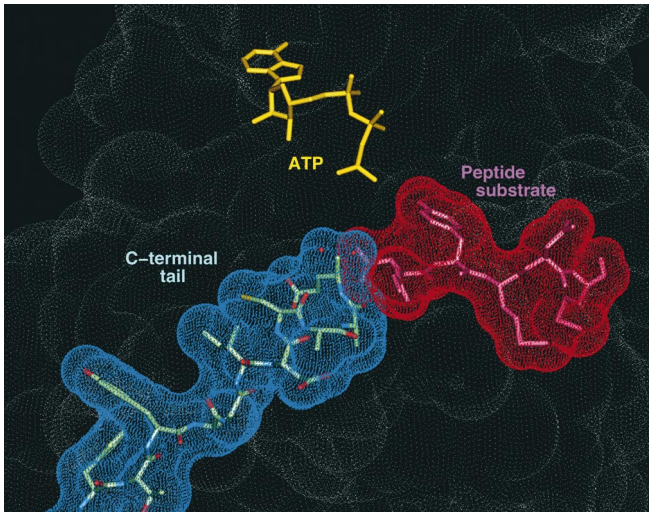

Figure 6. Proximity of the C-Terminal Tail to the Substrate Binding Site

Solvent-exposed surface representation of the Tie2K active site is shown in white. The surface of the C-terminal tail is shown in blue. ATP and peptide substrate from the activated IRK complex structure are modeled into the Tie2K active site by superimposing the C_αs of the C-terminal domain α helices. The surface of the peptide substrate is highlighted in red; ATP is shown in yellow. The figure was prepared with QUANTA.

dilated blood vessels that lack or have a reduced smooth-muscle layer and little to no supportive tissue. Receptor tyrosine kinases require the binding of an extracellular ligand to promote dimerization, autophosphorylation, and activation of the kinase domain (reviewed in [15]). These two mutations result in ligand-independent autophosphorylation and activation of Tie2 [19, 20]. Tie2 is able to autophosphorylate to its fully active state without ligand-mediated receptor dimerization. It has been suggested that these mutations either promote dimerization of the protein in the absence of an extracellular ligand or relieve autoinhibition of the kinase [19]. We have examined the structure of Tie2K in its unphosphorylated and monophosphorylated (Y897) states, as well as the activity of the wild-type and the Y897F/Y1048F/S119A mutant proteins, and we speculate on how the R849W and Y897S mutations might activate Tie2K activity.

Purified wild-type Tie2K, a significant fraction of which is phosphorylated on Y897, has a very low level of kinase activity and could not appreciably autophosphorylate Y992 in the activation loop. The Y897F/Y1048F/S119A mutant, on the other hand, could autophosphorylate Y992, and this ability led to an approximately 100-fold increase in kinase activity. Therefore, while the nonphosphorylated and monophosphorylated wild-type proteins and the Y897F/Y1048F/S119A mutant protein have identical crystal structures, Y897 influences the activity of the protein in solution.

Tie2K crystal forms I and II, which contain unphosphorylated protein, have two molecules in the asymmetric unit. The crystal form III, which contains monophosphorylated protein (Y897), contains only one molecule in the asymmetric unit. In the two unphosphorylated crystal forms, one crystal contact (approximately 1096 $Å^2$) is conserved at the noncrystallographic 2-fold axis (Figure 7). This contact primarily involves β1 but also residues from the ends of β2, β3, and β4 in the N-terminal domain. Residues R849 and Y897 sit at this crystal contact. F826, V829, and L839 form the hydrophobic core of this interface. Y897, Y899, R849, and D828 are located at the edges of the interface. R849, the first residue of β3, makes a weak hydrogen bond to Q837 of the neighboring molecule. The side chain of R849 is packed between the side chains of Y897 and V829 from the neighboring molecule. Y897 is located on the loop connecting β4 and β5 and packs against R849. Mutation of R849 to tryptophan may allow for better packing at this predominantly hydrophobic interface. On the other hand, phosphorylation of Y897 would be difficult to accommodate at this tight crystal contact and would therefore lead to crystal form III. If this crystal contact is in fact a biologically significant dimer interface, the phosphorylation state of Y897 may be another mechanism of controlling the activity of Tie2. When Y897 is phosphorylated, the cytoplasmic kinase domains cannot dimerize. However, when Y897 is unphosphorylated or mutated to a serine, Tie2K dimerization is favored.

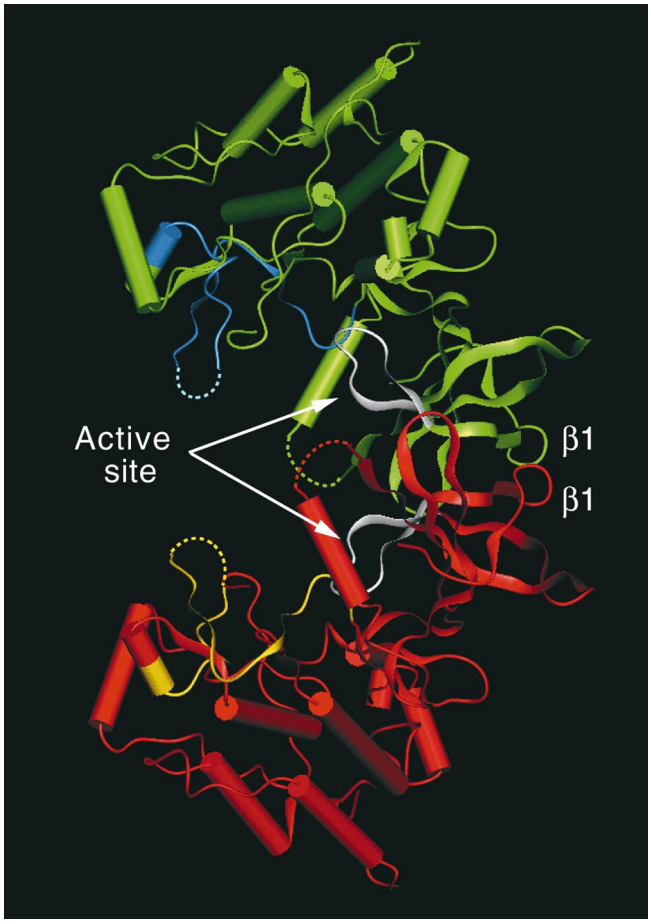

Figure 7. Noncrystallographic Dimer

The backbones of the two molecules in the asymetric unit are shown in red and green. The activation loops for molecules 1 and 2 are shown in yellow and blue. The nucleotide binding loops for both molecules are shown in white. The figure was prepared with QUANTA.

Alternatively, R849 and Y897 could influence Tie2 activity in vivo by interacting with accessory proteins. Phosphorylated Y897 has been shown to bind the SH2 domain of the protein tyrosine phosphatase Shp2 [36, 39]. This interaction may allow the phosphatase to dephosphorylate Y992 in the activation loop and therefore to downregulate the activity of the kinase. The R849W and Y897S mutations may disrupt the recognition

site for Shp2 or the kinase that phosphorylates Y897. Clearly, more experiments will be required to understand these mutations and the role of Y897 in kinase inhibition and/or activation.

Biological Implications

The crystal structure of unliganded Tie2K has revealed the structure of the kinase insert domain as well as several novel modes of self-inhibition. The position of the nucleotide binding loop and the Asp-Phe-Gly motif of the activation loop preclude ATP binding, while the C-terminal tail could block substrate binding. Phosphorylation of the N-terminal domain may serve as a negative regulatory mechanism by either preventing dimerization and autophosphorylation of the intracellular catalytic domains or recruiting a phosphatase. While the mechanisms by which Tie2 is activated for catalysis remain unclear, conformational changes in the nucleotide binding loop, the activation loops, the C-terminal tail, and C helix will all be required for both ATP and substrate binding. We are currently trying to crystallize Tie2K mutants in their activated form in order to understand the regulatory mechanisms of this kinase.

Experimental Procedures

Protein Expression

The cytoplasmic domain of Tie2 was cloned from a human kidney cDNA library (Clontech, Palo Alto, CA) by PCR. The sequence was identical to that reported in GenBank (L06139). The coding region corresponding to residues 808–1124 was subcloned into a pFASTBAC1 (GIBCO-BRL) expression vector by PCR. The N-terminal primer included an Sst1 restriction site and a methionine start codon followed by six histidine codons. The C-terminal primer included a stop codon and an Xho1 restriction site. The PCR product was cloned into the Sst1/XhoI site of pFASTBAC1. The Tie2K construct was transfected into *Spodoptera frugiperda* (Sf9) cells, single plaques were isolated, and high-titer stocks were generated. Sf9 cells were infected at a multiplicity of infection of 5 for 72 hr and harvested by centrifugation.

Protein Purification

Cells were resuspended in 50 mM HEPES (pH 8), 200 mM NaCl, and 20 mM imidazole and were disrupted by a polytron homogenizer and sonication. The homogenate was centrifuged for 40 min at 12,500 rpm. The supernatant was filtered (1.2 micron cartridge filter) and was loaded onto a Ni-chelating column (Pharmacia Chelating Sepharose FF). Protein was eluted with a 10 column volume linear gradient between 20 and 300 mM imidazole in 50 mM HEPES (pH 8) and 200 mM NaCl. Tie2K protein was pooled and loaded directly onto a hydroxylapatite column (BioRad Type I ceramic hydroxylapatite). A linear gradient was run from 0 to 100 mM potassium phosphate in 20 mM Tris-HCl (pH 8), 50 mM NaCl, 5 mM DTT, and 5% glycerol. The Tie2K-containing fractions were diluted 1:1 with 20 mM Tris-HCl (pH 8), 5 mM DTT, and 5% glycerol, loaded onto an anion exchange column (Pharmacia Q-Sepharose HP), and eluted with a 0–600 mM NaCl gradient. Tie2K was pooled based upon SDS-PAGE analysis (>95% purity) and stored at –80°C.

In Vitro Autophosphorylation for Mass Spectrometry

Wild-type and mutant Tie2K were incubated with 2 mM ATP and 10 mM $MgCl_2$ for 30 min at room temperature in 25 mM HEPES (pH 7.5), 150 mM NaCl, and 10 mM DTT. Samples were flash frozen and stored at −180°C until they could be analyzed by mass spectrometry.

In Vitro Kinase Assay

Nonactivated or preactivated Tie2K (10 nM) was used to phosphorylate 1 μM peptide substrate (Biotin-Ahx-LEARLVAYEGWVAGKKK-NH_2; Synpep, Dublin, CA) in the presence of 80 μM ATP, 10 mM $MgCl_2$, 1 mM DTT, 0.1 mg/ml BSA, and 0.1 M HEPES (pH 7.5). The reaction was carried out at room temperature for 30 min and then stopped by the addition of 50 mM EDTA. Streptavidin-APC (1.2 μg/ml) (Molecular Probes, Eugene, OR) and 0.15 μg/ml Eu-α-pY (EG&G Wallac, Gaithersburg, MD) in the presence of 0.1 mg/ml BSA and 0.1 M HEPES [pH7.5] were added, and the reactions were incubated for 10 min at room temperature. Streptavidin-APC and Eu-α-pY bind to the phosphorylated peptides to form a complex, allowing fluorescent energy transfer from Eu to APC. The plate was read on a Victor in time resolved–fluorescence mode by exciting at 340 nm and reading the emission at 665 nm.

Protein Digestion for Mass Spectrometry

Trypsin digestions of 200–1000 pmol of Tie2K were carried out in 50 mM Tris [pH 8.5], 1 mM $CaCl_2$, and 10% acetonitrile. In some instances, Tie2K was reduced and alkylated with DTT and 4-vinylpyridine prior to digestion. Digestion proceeded at 37°C for 12–18 hr.

Mass Spectrometry: LCMS

Mass measurements of intact protein were determined by using liquid chromatography mass spectrometry (LCMS). Protein samples were initially desalted on a Poros R2/H column (Perceptive Biosystems; Framingham, MA). Effluent from the desalting column was directed to a SCIEX API III mass spectrometer (PE Sciex, Concord, ON, Canada), and spectra were acquired in positive-ion mode with electrospray ionization. Intact protein mass values were obtained from the reconstructed mass spectra that were generated from the processed data. Assignment of phosphorylation states was made by identifying masses that were multiples of 80 Da higher than the expected mass of Tie2K.

Mass Spectrometry: NanoES MS

Nanoelectrospray ionization (nanoES) MS on a Q-TOF instrument from Micromass (UK) was used to map phosphorylation sites after trypsin digestion. Sample was introduced to the MS with either static nanoES using a pulled capillary tip (Mann) or capillary LCMS/MS. The LC system was from LC Packings and consisted of the Famos autosampler and the Ultimate solvent delivery pump. Separation was carried out on a 75 μm I.D. C18 PepMap column, also from LC Packings. The Q-TOF is capable of data dependent ion selection for collision-induced fragmentation.

Two sample preparation approaches were used to map the phosphorylation sites. In the first approach, phosphorylated peptides were isolated from nonphosphorylated peptides by using Ga(III) immobilized metal affinity chromatography (IMAC). Briefly, an aliquot of the trypsin digest was acidified and loaded onto an IMAC microcolumn charged with Ga(III). The column was then washed with 0.1% acetic acid/ 30% acetonitrile to remove nonphosphorylated peptides. Retained peptides were then eluted with 0.2 M sodium phosphate (pH 8.2) and directly applied to a microcolumn packed with Poros R2/H reverse-phase media. Bound peptides were washed with 0.1% formic acid and then eluted directly into a nanoelectrospray capillary tip. Static nanoESI was used to acquire MS and MS/MS spectra of the purified peptides. Phosphorylated residues were identified from MS/MS data.

In the second approach, the Tie2K trypsin digest was analyzed by capillary LCMS/MS with data-dependant scanning. This data file was then used to conduct a Mascot protein database search that compares uninterpreted MS/MS data to theoretical MS/MS spectra of user-specified proteolytic peptides. The spectra were interpreted manually to confirm the assignment.

Crystallization and Data Collection

All four crystal forms of Tie2K were grown by the hanging-drop vapor diffusion method. The protein (6 mg/ml in 20 mM HEPES [pH 7.5], 300 mM NaCl, 5 mM DTT) was mixed with an equal volume of reservoir and incubated at 22°C. The reservoir for crystal forms I and II was 2.5% PEG12000, 2.5% glycerol, 100 mM HEPES (pH 7.5), and 10 mM spermidine. The reservoir for crystal form III was 100 mM HEPES (pH 7.5), 100 mM KCl, and 10% isopropanol, while the reservoir for crystal form IV was 100 mM HEPES (pH 7.5) and 1.5 M NaCl. Crystals belonging to the four different space groups appeared within several days to several weeks and typically grew to approximately $100 \times 100 \times 10$ μm in 1–2 months. Glycerol was added to a final concentration of 25% as a cryoprotectant, and the crystals were flash frozen in liquid N_2.

Data for crystal forms I, II, and IV were collected at beamline 17-ID on a MAR-CCD in the facilities of the Industrial Macromolecular Crystallography Association Collaborative Access Team (IMCA-CAT) at the Advanced Photon Source. These facilities are supported by the companies of the Industrial Macromolecular Crystallography Association through a contract with Illinois Institute of Technology (IIT). This contract is executed through IIT's Center for Synchrotron Radiation Research and Instrumentation. The data were processed using HKL2000 [41]. Data for crystal form III was collected on an RAXIS4 image plate operating on a Rigaku rotating anode generator. The data were processed with DENZO and scaled with SCALEPACK [41].

Structure Determination and Refinement

The structure of crystal form I was solved first and was subsequently used to solve the other three crystal forms. The structure was solved by molecular replacement using CNS [42] and FGFR1 as a search model (molecule 1 of PDB entry 1FGK) [28]. The search model contained FGFR1 residues 464–485, 491–500, 506–578, 592–647 and 651–761. Residues not conserved between FGFR1 and Tie2 were truncated to alanine in the model. The correct solutions were the top two peaks in both the rotation and translation functions and had correlation coefficients of 0.38 and 0.36. Rigidbody refinement gave an R factor of 49%. Multiple rounds of model building and refinement were carried out with QUANTA [43] and CNS. The overall structure was confirmed by a composite omit map calculated with CNS. Residues 813, 858, 860, 867, 997, 1099, and 1119 were modeled as alanine in all four crystal forms due to a lack of side chain density. Structure analysis with PROCHECK indicated that all main chain torsions fall within the allowed regions of the Ramachandran plot [44].

Acknowledgments

We thank Dr. Masaaki Furuta for generating the Tie2K mutant, Wendy Liu for running the kinase assays, Drs. Shawn Willams and Robert Nolte for collecting the X-ray data at Argonne National Labs, and Drs. Lee Kuyper, Shawn Williams, and Steve Short for critical reading of the manuscript. Use of the Advanced Photon Source was supported by the US Department of Energy, Basic Energy Sciences, Office of Science, under contract number W-31-109-Eng-38.

Received: August 7, 2000
Revised: September 18, 2000
Accepted: September 22, 2000

References

1. Folkman, J., and Shing, Y. (1992). Angiogenesis. J. Biol. Chem. *267*, 10931–10934.
2. Risau, W. (1995). Differentiation of the endothelium. FASAB J. *9*, 926–933.
3. Pepper, M.S. (1996). Positive and negative regulation of angiogenesis: from cell biology to the clinic. Vasc. Med. *1*, 259–266.
4. Kuiper, R.A.J., Schellens, J.H.M., Blijham, G.H., Beijnen, J.H., and Voest, E.E. (1998). Clinical research on antiangiogenic therapy. Pharmacol. Res. *37*, 1–16.
5. Kumar, R., and Fidler, I.J. (1998). Angiogenic molecules and cancer metastasis. In Vivo *18*, 27–34.
6. Szekanecz, Z., Szegedi, G., and Koch, A.E. (1998). Angiogenesis in rheumatoid arthritis: pathogenic and clinical significance. J. Invest. Med. *46*, 27–41.
7. Tolentino, M.J., and Adamis, A.P. (1988). Angiogenic factors in the development of diabetic iris neovascularization and retinopathy. Int. Ophthalmol. Clin. *38*, 77–94.
8. Tallquist, M.D., Soriano, P., and Klinghoffer, R.A. (1999). Growth factor signaling pathways in vascular development. Oncogene *18*, 7917–7932.
9. Merenmies, J., Parada, L.F., and Henkemeyer, M. (1997). Receptor tyrosine kinase signaling in vascular development. Cell Growth Differ. *8*, 3–10.
10. Ferrara, N., and Davis-Smyth, T. (1997). The biology of vascular endothelial growth factor. Endocrine Rev. *18*, 4–25.
11. Borgström, P., Hillan, K.J., Sriranarao, P., and Ferrara, N. (1996). Complete inhibition of angiogenesis and growth of microtumors by anti-vascular endothelial growth factor neutralizing antibodies. Novel concepts of angiostatic therapy from intravital videomicroscopy. Cancer Res. *56*, 4032–4039.
12. Adamis, A.P., et al., and Miller, J.W. (1996). Inhibition of VEGF prevents retinal ischemia-associated iris neovascularization in a primate. Arch. Ophthalmol. *114*, 66–71.
13. Koblizek, T.I., Weiss, C., Yancopoulos, G.D., Deutsch, U., and Risau, W. (1998). Angiopoietin-1 induces sprouting angiogenesis *in vitro*. Curr. Biol. *8*, 529–532.
14. Witzenbichler, B., Maisonpierre, P.C., Jones, P., Yancopoulos, G.D., and Isner, J.M. (1998). Chemotactic properties of angiopoietin-1 and -2, ligands for the endothelial-specific receptor tyrosine kinase Tie2. J. Biol. Chem. *273*, 18514–18521.
15. Lemmon, M.A., and Schlessinger, J. (1994). Regulation of signal transduction and signal diversity by receptor oligomerization. Trends Biochem. Sci *19*, 459–463.
16. Davis, S., et al., and Yancopoulos, G.D. (1996). Isolation of angiopoietin-1, a ligand for the TIE2 receptor, by secretion-trap expression cloning. Cell *87*, 1161–1169.
17. Maisonpierre, P.C., et al., and Yancopoulos, G.D. (1997). Angiopoietin-2, a natural antagonist for Tie2 that disrupts *in vivo* angiogenesis. Science *277*, 55–60.
18. Valenzuela, D.M., et al., and Yancopoulos, G.D. (1999). Angiopoietins 3 and 4: diverging gene counterparts in mice and humans. Proc. Natl. Acad. Sci. USA *96*, 1904–1909.
19. Vikkula, M., et al., and Olsen, B.R. (1996). Vascular Dysmorphogenesis caused by an activating mutation in the receptor tyrosine kinase Tie2. Cell *87*, 1181–1190.
20. Calvert, J.T., et al., and Marchuk, D.A. (1999). Allelic and locus heterogeneity in inherited venous malformations. Hum. Mol. Genet. *8*, 1279–1289.
21. Sato, T.N., et al., and Qin, Y. (1995). Distinct roles of the receptor tyrosine kinases Tie-1 and Tie-2 in blood vessel formation. Nature *376*, 70–74.
22. Dumont, D.J., et al., and Breitman, M.L. (1994). Dominant-negative and targeted null mutations in the endothelial receptor tyrosine kinase, tek, reveal a critical role in vasculogenesis of the embryo. Genes Dev. *8*, 1897–1909.
23. Suri, C., et al., and Yancopoulos, G.D. (1996). Requisite role of angiopoietin-1, a ligand for the TIE2 receptor, during embryonic angiogenesis. Cell *87*, 1171–1180.
24. Suri, C., et al., and Yancopoulos, G.D. (1998). Increased vascularization in mice overexpressing angiopoietin-1. Science *282*, 468–471.
25. Lin, P., et al., and Peters, K.G. (1998). Antiangiogenic gene therapy targeting the endothelium-specific receptor tyrosine kinase Tie2. Proc. Natl. Acad. Sci. USA *95*, 8829–8834.
26. Hubbard, S.R., Wei, L., Ellis, L., and Hendrickson, W.A. (1994). Crystal structure of the tyrosine kinase domain of the human insulin receptor. Nature *372*, 746–754.
27. Hubbard, S.R. (1997). Crystal structure of the activated insulin receptor tyrosine kinase in complex with peptide substrate and ATP analog. EMBO J. *16*, 5572–5581.
28. Mohammadi, M., Schlessinger, J., and Hubbard, S.R. (1996). Structure of the FGF receptor tyrosine kinase domain reveals a novel autoinhibitory mechanism. Cell *86*, 577–587.
29. McTigue, M.A., et al., and Appelt, K. (1999). Crystal structure of the kinase domain of human vascular endothelial growth factor receptor 2: a key enzyme in angiogenesis. Structure *7*, 319–330.
30. Johnson, L.N., Noble, M.E.M., and Owen, D.J. (1996). Active and inactive protein kinases: structural basis for regulation. Cell *85*, 149–158.
31. Cox, S., Radzio-Andzelm, E., and Taylor, S.S. (1994). Domain movements in protein kinases. Curr. Opin. Struct. Biol. *4*, 893–901.
32. Knighton, D.R., et al., and Sowadski, J.M. (1991). Crystal structure of the catalytic subunit of cyclic adenosine monophosphate-dependent protein kinase. Science *253*, 407–413.
33. Jeffrey, P.D., et al., and Pavletich, N.P. (1995). Mechanism of CDK activation revealed by the structure of a cyclinA-CDK2 complex. Nature *376*, 313–320.
34. Heidaran, M.A., et al., and Aaronson, S.A. (1991). Deletion or substitution within the platelet-derived growth factor receptor kinase insert domain: effects on functional coupling with intracellular signaling pathways. Mol. Cell. Biol. *11*, 134–142.
35. Taylor, G.R., Reedijk, M., Rothwell, V., Rohrschneider, L., and Pawson, T. (1989). The unique insert of cellular and viral fms protein tyrosine kinase domains is dispensible for enzymatic and transforming activities. EMBO J. *8*, 2029–2037.
36. Huang, L., Turck, C.W., Rao, P., and Peters, K.G. (1995). GRB2 and SH-PTP2: potentially important endothelial signaling molecules downstream of the TEK/TIE2 receptor tyrosine kinase. Oncogene *11*, 2097–2103.
37. Jones, N., and Dumont, D.J. (1998). The Tek/Tie2 receptor signals through a novel Dok-related docking protein, Dok-R. Oncogene *17*, 1097–1108.
38. Kontos, C.D., et al., and Peters, K.G. (1998). Tyrosine 1101 of Tie2 is the major site of association of p85 and is required for activation of phosphatidylinositol 3-kinase and Akt. Mol. Cell. Biol. *18*, 4131–4140.
39. Jones, N., et al., and Dumont, D.J. (1999). Identification of Tek/Tie2 Binding Partners. J. Biol. Chem. *274*, 30896–30905.
40. Korpelainen, E.I., Karkkainen, M., Gunji, Y., Vikkula, M., and Alitalo, K. (1999). Endothelial receptor tyrosine kinases activate the STAT signaling

pathway: mutant Tie-2 causing venous malformations signals a distinct STAT activation response. Oncogene *18*, 1–8.

41. Otwinowski, Z. (1993). Oscillation data reduction program. In Proceedings of the CCP4 Study Weekend: Data Collection and Processing, L. Sawyer, N. Isaacs, and S. Bailey, eds. (England: SERC Daresbury Laboratory), pp. 56–62.
42. Brunger, A.T., et al., and Warren, G.L. (1998). Crystallography and NMR system: a new software suite for macromolecular structure determination. Acta. Crystallogr. D *54*, 905–921.
43. Quanta (1994). (San Diego, CA: Molecular Simulations).
44. Laskowski, R.A., MacArthur, M.W., Moss, D.S., and Thornton, J.M. (1993). PROCHECK: a program to check the stereochemical quality of protein structures. J. Appl. Crystallogr. *26*, 283–291.
45. Carson, M., and Bugg, C.E. (1986). Algorithm for Ribbon Models of Proteins. J. Mol. Graphics *4*, 121–122.
46. Nicholls, A., Sharp, K.A., and Honig, B. (1991). Protein folding and association: insights from the interfacial and thermodynamic properties of hydrocarbons. Proteins *11*, 281–296.